https://doi.org/10.5194/os-2020-65
Preprint. Discussion started: 3 July 2020
© Author(s) 2020. CC BY 4.0 License.

Ocean Science
Discussions
Open Access
EGU

A mosaic of phytoplankton responses across Patagonia, the SE Pacific and SW Atlantic Ocean to ash deposition and trace metal release from the Calbuco 2015 volcanic eruption

Maximiliano J. Vergara-Jara[1,2], Mark J. Hopwood[3*], Thomas J. Browning[3], Insa Rapp[4], Rodrigo Torres[2,5], Brian Reid[5], Eric P. Achterberg[3], José Luis Iriarte[2,6].

[1]Programa de Doctorado en Ciencias de la Acuicultura, Universidad Austral de Chile, Puerto Montt, Chile.
[2]Instituto de Acuicultura & Centro de Investigación Dinámica de Ecosistemas Marinos de Altas Latitudes - IDEAL, Universidad Austral de Chile, Puerto Montt, Chile.
[3]GEOMAR, Helmholtz Centre for Ocean Research, 24148 Kiel, Germany.
[4]Department of Biology, Dalhousie University, Halifax, Nova Scotia, Canada
[5]Centro de Investigación en Ecosistemas de la Patagonia (CIEP), Coyhaique, Chile.
[6]COPAS-Sur Austral, Centro de Investigación Oceanográfica en el Pacífico Sur-Oriental (COPAS), Universidad de Concepción, Concepción, Chile.

Key words: volcanic ash, iron, Fe(II), phytoplankton, carbonate chemistry, Reloncaví Fjord

Corresponding author*: mhopwood@geomar.de

https://doi.org/10.5194/os-2020-65
Preprint. Discussion started: 3 July 2020
© Author(s) 2020. CC BY 4.0 License.


Ocean Science
Discussions
Open Access
EGU

38 **Abstract**

39 Following the April 2015 eruption of the Calbuco volcano, an extensive ash plume spread
40 across northern Patagonia and into the SE Pacific and SW Atlantic Ocean. Here we report
41 the results of field surveys conducted in the marine region receiving the highest ash load
42 following the eruption (Reloncaví Fjord). The fortuitous location of a long-term monitoring
43 station in Reloncaví Fjord provided data to evaluate inshore phytoplankton bloom dynamics
44 and carbonate chemistry during April-May 2015. Satellite derived chlorophyll-a
45 measurements over the ocean regions affected by the ash plume in May 2015 were obtained
46 to determine the spatial-temporal gradient in offshore phytoplankton response to ash.
47 Additionally, leaching experiments were performed to quantify the release of total alkalinity,
48 trace elements (Fe, Mn, Pb, Co, Cu, Ni and Cd) and major ions (Fl, Cl, SO_4, NO_3, Li, Na,
49 NH_4, K, Mg, Ca) from ash into solution. Within Reloncaví Fjord, integrated peak diatom
50 abundances during the May 2015 austral bloom were higher than usual (up to 1.4×10^{11} cells
51 m^{-2}, integrated to 15 m depth), with the bloom intensity perhaps moderated due to high ash
52 loadings in the two weeks following the eruption. In the offshore SE Pacific, a short duration
53 phytoplankton bloom corresponded closely in space and time to the maximum observed ash
54 plume, potentially in response to Fe-fertilization of a region where phytoplankton growth is
55 typically Fe-limited at this time of year. Conversely, no clear fertilization was found in the
56 area subject to an ash plume over the SW Atlantic where the availability of fixed nitrogen is
57 thought to limit phytoplankton growth which was consistent with no significant release of
58 fixed nitrogen from ash.

59

60 In addition to release of nanomolar concentrations of dissolved Fe from ash suspended in
61 seawater, it was observed that low loadings (< 5 mg L^{-1}) of freshly deposited ash were an

https://doi.org/10.5194/os-2020-65
Preprint. Discussion started: 3 July 2020
© Author(s) 2020. CC BY 4.0 License.

Ocean Science
Discussions
Open Access
EGU

62 unusually prolific source of Fe(II) into solution (up to 1.0 μmol Fe g^{-1}), suggesting that the
63 release of bioaccessible Fe from ash sources may generally be under-estimated when
64 quantified from aged ash. This release of Fe(II) may make freshly deposited ash an unusually
65 efficient dissolved Fe source with the 18-38% fraction of dissolved Fe released as Fe(II) from
66 Calbuco ash roughly comparable to literature values for Fe released into seawater from
67 aerosols collected over the Pacific Ocean.

https://doi.org/10.5194/os-2020-65
Preprint. Discussion started: 3 July 2020
© Author(s) 2020. CC BY 4.0 License.

Ocean Science
Discussions
Open Access
EGU

1. Introduction

Volcanic ash has long been considered a large, intermittent source of trace metals to the ocean (Frogner et al., 2001; Sarmiento, 1993; Watson, 1997) and its deposition is now deemed a sporadic generally low-macronutrient, high-micro-nutrient supply mechanism (Ayris and Delmelle, 2012; Jones and Gislason, 2008; Lin et al., 2011). As volcanic ash can be a regionally significant source of allochthonous inorganic material to affected water bodies, volcanic eruptions have the potential to dramatically change light availability, the carbonate system, properties of sinking particles and ecosystem dynamics in impacted waterbodies (Hoffmann et al., 2012; Newcomb and Flagg, 1983; Stewart et al., 2006). Surveys directly underneath the ash plume from the 2013 eruption of Eyjafjallajökull (Iceland) over the North Atlantic found, among other biogeochemical perturbations, high dissolved Fe (dFe) concentrations of up to 10 nM in affected surface seawater (Achterberg et al., 2013) which could potentially result in enhanced primary production. The greatest potential positive effect of ash on marine productivity would therefore generally be expected in high-nitrate, low-chlorophyll (HNLC) areas of the ocean (Hamme et al., 2010; Mélançon et al., 2014), where low Fe concentrations are a major factor limiting primary production (Martin et al., 1990; Moore et al., 2013). Special interest is therefore placed on the ability of volcanic ash to release dFe, and other bio-essential trace metals such as Mn (Achterberg et al., 2013; Browning et al., 2014; Hoffmann et al., 2012), into seawater. Conversely, apart from inducing light limitation, other negative effects of ash deposition on marine organisms could arise from metal toxicity (Ermolin et al., 2018)- particularly when dust loading is high (Hoffmann et al., 2012)- or more generally from the ingestion of ash particles by filter feeders, phagotrophic organisms or fish (Newcomb and Flagg, 1983; Wolinski et al., 2013). Transient shifts to low pH have also been reported in some, but not all, ash leaching

https://doi.org/10.5194/os-2020-65
Preprint. Discussion started: 3 July 2020
© Author(s) 2020. CC BY 4.0 License.


92 experiments and in some natural waterbodies following intense ash falls, suggesting that
93 perturbations to the carbonate system are a further impact of volcanic ash in aquatic
94 environments (Duggen et al., 2010; Jones and Gislason, 2008; Newcomb and Flagg, 1983).
95 The greatest negative impact of ash on primary producers would therefore be expected closest
96 to source where the ash loading is highest and in areas where macronutrients or light, rather
97 than trace elements, limit primary production.
98
99 In contrast to the North Atlantic 2013 Eyjafjallajökull plume over the North Atlantic, the
100 2015 ash plume from the Calbuco eruption (northern Patagonia, Chile) was predominantly
101 deposited largely over an inshore and coastal region (Romero et al., 2016). This led to visible
102 high ash loadings in affected surface waters in the weeks after the eruption, providing a case
103 study for a concentrated ash deposition event in a coastal system; Reloncaví Fjord, which is
104 the northernmost fjord of Patagonia. It receives the direct discharge of three major rivers,
105 creating a highly stratified and productive fjord system in terms of both phytoplankton
106 biomass and aquaculture production of mussels (González et al., 2010; Molinet et al., 2017;
107 Yevenes et al., 2019). Here we combine in situ observations from moored arrays which were
108 fortuitously deployed in Reloncaví Fjord (Vergara-Jara et al., 2019), with satellite-derived
109 chlorophyll data for offshore regions subject to ash deposition, and leaching experiments to
110 investigate the inorganic consequences of ash addition to solution. We thereby evaluate the
111 potential positive and negative effects of ash from the 2015 Calbuco eruption on marine
112 primary production in three geographical regions; Reloncaví Fjord and the areas of the SE
113 Pacific and SW Atlantic Ocean beneath the most intense ash plume.
114
115

https://doi.org/10.5194/os-2020-65
Preprint. Discussion started: 3 July 2020
© Author(s) 2020. CC BY 4.0 License.

2. **Materials and methods**

2.1. *Study area*

The Calbuco volcano (Fig. 1) is located in a region with large freshwater reservoirs and a major river (the Petrohué) that flows into Reloncaví Fjord. The predominant bedrock type is andesite (López-Escobar et al., 1995). Reloncaví Fjord is 55 km long and receives freshwater from 3 main rivers, the Petrohué, Cochamó and Puelo, with mean monthly streamflows of 350 $m^3 s^{-1}$, 100 $m^3 s^{-1}$ and 650 $m^3 s^{-1}$, respectively (León-Muñoz et al., 2013). River discharge strongly influences seasonal patterns of primary production across the region, supplying silicic acid and strongly stratifying the water column (Castillo et al., 2016; González et al., 2010; Torres et al., 2014). Seasonal changes in light availability rather than macronutrient supply are thought to control marine primary production across the Reloncaví region with marine primary production high (>1 g C m^{-2} day^{-1}) throughout austral spring, summer and early autumn (González et al., 2010).

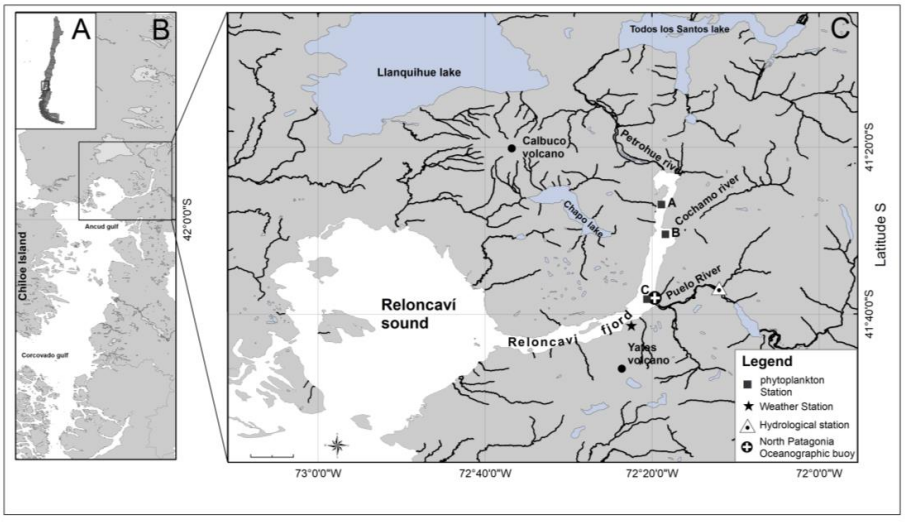

Figure 1. The Calbuco region showing the location of Reloncaví Fjord, 3 major rivers (Petrohué, Cochamó and Puelo) discharging into the fjord, the 3 stations (black squares; A,

https://doi.org/10.5194/os-2020-65
Preprint. Discussion started: 3 July 2020
© Author(s) 2020. CC BY 4.0 License.


132 B and C) used to assess changes in phytoplankton abundance following the eruption, a
133 hydrological station that monitors Puelo river flow, a weather station and the location of a
134 long-term mooring within the fjord.
135
136 On 22 April 2015 the Calbuco volcano erupted after 54 years of dormancy. Two major
137 eruption pulses lasted <2 hours on 22 April and 6 hours on 23 April, releasing a total volume
138 of 0.27 km^3 ash which was projected up to 20 km height above sea level (Van Eaton et al.,
139 2016; Romero et al., 2016). Ash layers several cm thick were deposited mainly to the NE of
140 the volcano in subsequent days (Romero et al., 2016). Fortuitously, as part of a long-term
141 deployment, an ocean acidification buoy in the middle of Reloncaví Fjord (Vergara-Jara et
142 al., 2019) and an associated meteorological station close to the volcano (Fig. 1) were well
143 placed to assess the impact of ash fall immediately after the eruption. To compliment data
144 from these facilities, after the evacuation order was removed, weekly sampling campaigns
145 were conducted in the fjord commencing one week after the eruption.
146
147 **2.2. Ash samples – trace metal leaching experiments**

148 Ash (500 g) was collected (6 May 2015, in Cochamó, Chile) from the surface of a plastic
149 container using plastic sheeting, double sealed in low density polyethylene (LDPE) plastic
150 bags and stored in the dark. A sub-sample was analyzed for particle size using a Mastersizer
151 2000 at The University of Chile. South Atlantic seawater for incubation experiments was
152 collected using a towfish and trace metal clean tubing in a 1 m^3 high density polyethylene
153 tank which had been pre-rinsed with 1 M HCl. This water was stored in the dark for >12
154 months prior to use in leaching experiments. All labware for trace metal leaching experiments

https://doi.org/10.5194/os-2020-65
Preprint. Discussion started: 3 July 2020
© Author(s) 2020. CC BY 4.0 License.

Ocean Science
Discussions
Open Access
EGU

was pre-cleaned with Mucasol and 1 M HCl. 125 ml LDPE bottles (Nalgene) for trace metal leach experiments were pre-cleaned using a 3-stage procedure with three de-ionized water (Milli-Q, Millipore, conductivity 18.2 MΩ cm^{-1}) rinses after each stage (Mucasol, 1 week in 1 M HCl, 1 week in 1 M HNO_3).

Leach experiments were conducted by adding a pre-weighed mass of ash into 100 ml South Atlantic Seawater, gently mixing the suspension for 10 minutes, and then syringe filtering the suspension (0.2 µm, polyvinylidene fluoride, Millipore). Eight different ash loadings from 2-50 mg L^{-1} were used, with each treatment run in triplicate. Samples for dissolved trace metals (Fe, Cd, Pb, Ni, Cu, Co and Mn) were acidified within 1 day of collection by the addition of 140 µL HCl (UPA grade, ROMIL) and analysed by inductively coupled plasma mass spectroscopy following preconcentration exactly as per Rapp et al., (2017).

Leach experiments specifically to measure Fe(II) release were conducted in a similar manner. A pre-weighed mass of ash was added into 250 ml South Atlantic seawater and shaken by hand for approximately one minute. Ash loadings ranged from 0.2-4000 mg L^{-1}. Fe(II) was then measured via flow injection analysis using luminol chemiluminescence (Jones et al., 2013) without pre-concentration or filtration. The inflow line feeding the flow injection apparatus was positioned inside the ash suspension immediately after mixing and measurements begun thereafter at 2 minutes resolution. Reported values are the mean (± standard deviation) Fe(II) concentrations measured from 2-30 minutes after adding ash into solution. Calibrations were run daily using standard additions of Fe(II) to aged (unfiltered) South Atlantic seawater. After dissolution experiments the apparatus was rinsed with 0.1 M HCl (reagent grade) followed by flushing with de-ionized water to ensure the removal of ash particles. In addition to dissolution experiments using Calbuco ash, for comparative

https://doi.org/10.5194/os-2020-65
Preprint. Discussion started: 3 July 2020
© Author(s) 2020. CC BY 4.0 License.


purposes, suspensions of the following particles were also tested for Fe(II) release: volcanic ash retained from past eruptions (2002/Etna and 2008/Chaitén), dessert derived aerosols, glacial flour, iceberg borne particles and basalt/peridotite reference materials (see Supplementary Table).

2.3 Ash samples - Fresh and brackish water leaching experiments for total alkalinity, ion and nutrient measurements

Both brackish sub-surface water from the study region (Aysén Fjord, salinity 16.3), and de-ionized water were used for leaching experiments following the recommendations of Witham et al., (2005). Leaches were conducted in 50 ml LDPE bottles filled with either 40 ml brackish or fresh water with 4 replicates of each treatment. Bottles were incubated inside a mixer at room temperature after the addition of 0.18 g ash, using two ash size fractions (<63 μm and 250-1000 μm) which were separated using sieves (ASTM e-11 specification, W.S. Tyler). The sampling times were at time zero (defined as just after the addition of the ash and a few minutes of mixing), 2 h and 24 h later. Samples were immediately analyzed for total alkalinity (A_T). Leaching experiments conducted with brackish water were analyzed for A_T via a potentiometric titration using reference standards (Haraldsson et al., 1997) ensuring a reproducibility < 2 μmol/kg. For the de-ionized water leaching experiment, A_T was analyzed by titration of unfiltered 5 ml subsamples to a pH 4.5 endpoint (Bromocresol Green/Methyl Red) using a Dosimat (Metrohm Inc) and 0.02 N H_2SO_4 titrant. Alkalinity was calculated as $CaCO_3$ equivalents following APHA 2005-Methods 2320. Additional 5 ml subsamples were filtered, stored at 4°C and analyzed within 3 days for major ions (Fl, Cl, SO_4, NO_3, Li, Na, NH_4, K, Mg, Ca) using a DionexTM 5000 Ion Chromatography system with Eluent Generation (APHA). All measurements were then corrected for initial water concentrations

https://doi.org/10.5194/os-2020-65
Preprint. Discussion started: 3 July 2020
© Author(s) 2020. CC BY 4.0 License.


prior to ash addition.

2.4 Environmental data – continuous Reloncaví Fjord monitoring

High temporal resolution (hourly) in situ measurements were taken simultaneously at the surface and at 3 m depth for pCO_2, pH, depth, temperature, conductivity and dissolved O_2 using two SAMI sensors that measured spectrophotometric CO_2 and pH (DeGrandpre et al., 1995; Seidel et al., 2008) (Sunburst Sensors, LLC), and an SBE 37 MicroCAT CTD-ODO (SeaBird Electronics) for temperature, conductivity, depth and dissolved O_2. Identical sets of instruments were deployed at the surface of Reloncaví Fjord and also at 3 m depth as per Vergara-Jara et al., (2019). Sensor maintenance and quality control is described by Vergara-Jara et al., (2019). The error in pCO_2 concentrations is estimated to be at most 5% which arises mainly due to a non-linear sensor response and reduced sensitivity at high pCO_2 levels >1500 ppm (DeGrandpre et al., 1999). The SAMI-pH instruments used an accuracy test instead of a calibration procedure (Seidel et al., 2008). With the broad pH and salinity range found in the fjord, pH values are subject to a maximum error of ±0.02 (Mosley et al., 2004).

A meteorological station (HOBO-U30, Fig. 1) measured air temperature, solar radiation, wind speed and direction, rainfall, and barometric pressure every 5 minutes. Puelo River streamflow was obtained from the Carrera Basilio hydrological station (Fig. 1), run by Dirección General de Aguas de Chile (http://snia.dga.cl/BNAConsultas/reportes).

2.5 Field surveys in Reloncaví Fjord post eruption

During May 2015, weekly field campaigns were undertaken in the Reloncaví Fjord. Phytoplankton samples were collected at 3 depths for taxonomic characterization and

https://doi.org/10.5194/os-2020-65
Preprint. Discussion started: 3 July 2020
© Author(s) 2020. CC BY 4.0 License.


abundance determination (1 m, 5 m and 10 m) at 3 stations (A, B and C; Fig. 1) using a 5 L Go-Flo bottle. Samples were analyzed using a Olympus CKX41 inverted phase contrast microscope using a 10 ml sedimentation chamber and the Utermöhl method (Utermöhl, 1958). The phytoplankton community composition was then statistically analyzed in R (RStudio V 1.2.5033) using general linear models in order to find statistically significant differences between dates and group abundances. Additionally, as part of a long-term monitoring program at station C (Fig. 1), on 6 occasions during March-May 2015, chlorophyll-a samples were retained from 6 depths (1, 3, 5, 7, 10 and 15 m). Chlorophyll-a was determined after filtering 250 ml onto GFF filters (Whatman) by fluorometry as per Welschmeyer (1994). Integrated chlorophyll-a (mg m^{-2}) and diatom abundance (cells m^{-2}) was determined to 15 m depth. Chlorophyll-a within Reloncaví Fjord is invariably concentrated in the upper 10-15 m (González et al., 2010; Yevenes et al., 2019). Two additional profiles close to Station C were obtained from Yevenes et al., (2019).

2.6 Satellite data

Daily, 4 km resolution chlorophyll-a images from the MODIS Aqua sensor (OCI algorithm; Hu et al., 2012) were downloaded from the NASA Ocean Color website (https://oceancolor.gsfc.nasa.gov) for the period 4 April 2015–2 May 2015. As a proxy for the spatial extent and loading of the ash plume, the UV aerosol index product from the Ozone Monitoring Instrument (OMI) on the EOS-Aura was downloaded for the same time period. Daily images were composited into 5-day mean averages (Fig. 7).

https://doi.org/10.5194/os-2020-65
Preprint. Discussion started: 3 July 2020
© Author(s) 2020. CC BY 4.0 License.

3. Results

3.1 In situ observations

The Calbuco ash plume reached up to 20 km height and was dispersed hundreds of kilometers across Patagonia and the Pacific and Atlantic Oceans (Fig. 2). The ash loading in water bodies near the cone was visually observed to be high, especially near the Petrohué river catchment that drains into the head of the Reloncaví fjord. This ash loading into the fjord was clearly visible on 6 May 2015 when ash samples were collected for leach experiments (Fig. 2).

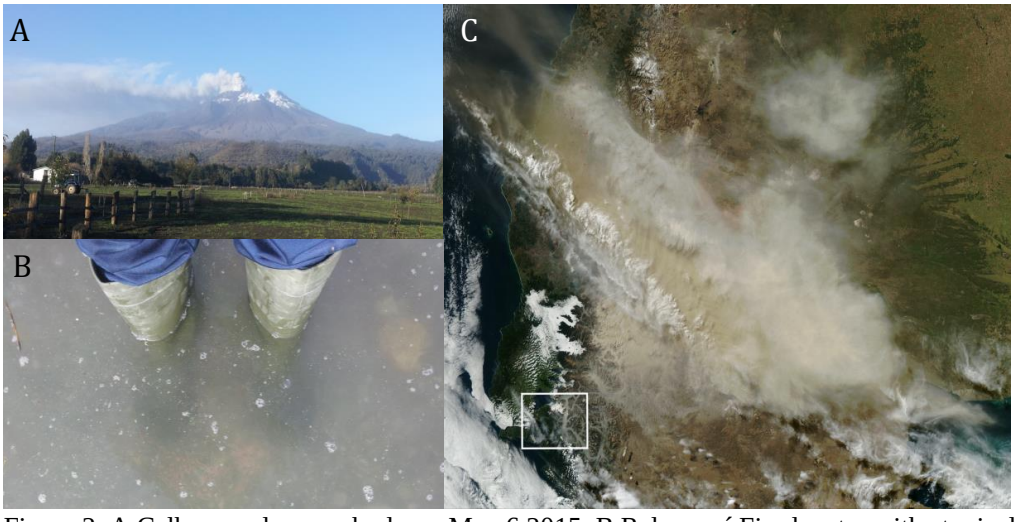

Figure 2. A Calbuco volcano ash plume May 6 2015. B Reloncaví Fjord water with atypical high turbidity due to the ash loading, Cochamó town 6 May 2015. C Ash cloud visible on MODIS Aqua satellite from the NASA Earth Observatory, April 23 (http://earthobservatory.nasa.gov/NaturalHazards/view.php?id=85767&eocn=home&eoci=nh). The highlighted box in C corresponds to Fig. 1 C.

https://doi.org/10.5194/os-2020-65
Preprint. Discussion started: 3 July 2020
© Author(s) 2020. CC BY 4.0 License.

Ocean Science
Discussions
Open Access
EGU

260

261

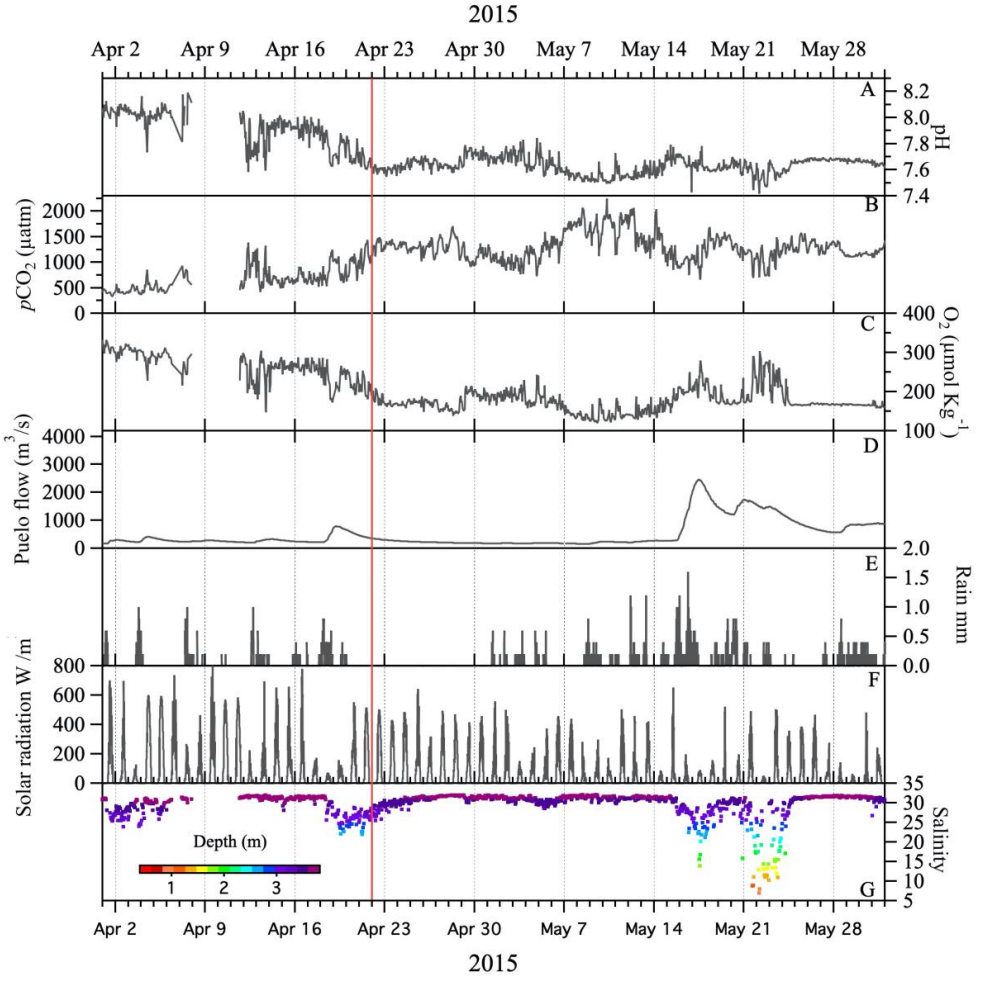

262

263 Figure 3 Continuous data from the Reloncaví Fjord mooring and nearby hydrological and
264 weather stations for April-May 2015. The vertical red line marks the eruption date. All
265 locations are marked in Fig 1. Carbonate chemistry and salinity data from Vergara-Jara et
266 al., (2019). Wind and tidal mixing causes small changes in the depth of the 'surface' sensor
267 which are shown alongside the salinity data.

https://doi.org/10.5194/os-2020-65
Preprint. Discussion started: 3 July 2020
© Author(s) 2020. CC BY 4.0 License.


268

269 Carbonate chemistry data from the Reloncaví Fjord mooring demonstrated that pH declined
270 and pCO_2 increased in the week prior to the eruption (22 April, Fig. 3). Oxygen and pH
271 reached a minimum and pCO_2 a maximum during the time period May 7-14, which indicates
272 a state of high respiration. In this stratified environment, the brackish fjord surface layer is
273 generally low pH, high pCO_2 with seasonal changes in salinity and respiration leading to a
274 large annual range of pCO_2 and pH (Vergara-Jara et al., 2019). The depth of the sensors
275 changed temporally due to changes in tides and river flow. This accounts for some of the
276 variation in measured salinity due to the strong salinity gradient with depth in the brackish
277 surface waters (Fig. 3). Any changes to pCO_2 or pH occurring as a direct result of the
278 eruption, or associated ash deposition, are therefore challenging to distinguish from
279 background variation as part of short-term (intra-day) or seasonal shifts in the carbonate
280 system which are pronounced in this dynamic and strongly freshwater influenced
281 environment (Fig. 3). Freshwater discharge from the Puelo increased sharply from May 16
282 which is an annually recurring event (González et al., 2010).

283

284

285

286

287

288

289

290

291

https://doi.org/10.5194/os-2020-65
Preprint. Discussion started: 3 July 2020
© Author(s) 2020. CC BY 4.0 License.

292 **3.2 Phytoplankton in Reloncaví fjord post-eruption**

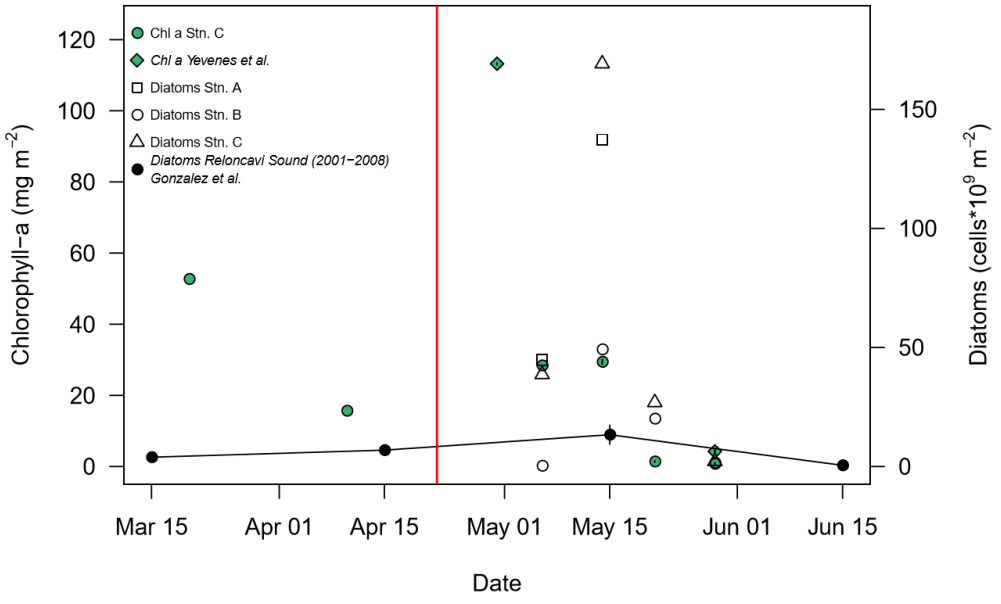

293

294 Figure 4. Changes in integrated (0-15 m) diatom abundance and chlorophyll-a for Reloncaví
295 Fjord in April-May 2015. Locations as per Fig. 1, the eruption date (22 April) is marked with
296 a red line. Historical diatom data from Reloncaví Sound (2001-2008, integrated to 10 m
297 depth, mean ± standard error, González et al., 2010) and additional chlorophyll data from
298 2015 ('Station 3' from Yevenes et al., 2019, approximately corresponding to Station C
299 herein) are also shown.

300

301 Phytoplankton abundances observed in May 2015 within Reloncaví Fjord assessed by diatom
302 cell counts and chlorophyll-a concentration were comparable to, or higher than, those
303 previously measured in the region (Fig. 4). Diatom abundance integrated to 15 m depth
304 peaked at Stations B and C on 16 May, with notably lower abundances at the more freshwater
305 influenced station A (Fig. 4). Chlorophyll-a concentrations at Station C, including two nearby

https://doi.org/10.5194/os-2020-65
Preprint. Discussion started: 3 July 2020
© Author(s) 2020. CC BY 4.0 License.


306 measurements from Yevenes et al., (2019), peaked on 30 April and declined to much lower
307 concentrations in June which is expected from patterns in regional primary production
308 (González et al., 2010). No measurements were available for 10-30 April 2015 (Fig. 4) and
309 thus it is not possible to determine the timing of the onset of the austral autumn phytoplankton
310 bloom with respect to the volcanic eruption from the available chlorophyll-a or diatom data.
311 Within this time period, the mooring at Station C (Fig. 3) however did record a modest
312 increase in pH and O_2 from 28-29 April, during a time period when river discharge and
313 salinity were stable, which could be indicative of the autumn phytoplankton bloom onset.
314

315 **3.3 Total alkalinity and macronutrients in leach experiments**

316 Size analysis of the collected ash determined a mean particle diameter of 339 µm. Small ash-
317 particles (<63 µm) resulted in minor, or no significant, changes to A_T in brackish fjord waters
318 (Fig. 5). With large ash-particles (>1.0 mm) any effect was even less evident. Conversely, a
319 leaching experiment with de-ionized water showed a small increase in A_T (Fig. 5). By
320 increasing the A_T of freshwater, ash would theoretically act to increase the buffering capacity
321 of river outflow into a typically weak carbonate system like the Reloncaví Fjord (Vergara-
322 Jara et al., 2019). However, the absolute change in A_T was relatively small despite the large
323 ash loading used in all incubations (< 20 µmol kg^{-1} A_T for ash loading >4 g L^{-1}) and therefore
324 it is expected that the direct effect of ash on A_T in situ was limited. Other effects on carbonate
325 chemistry may however arise due to ash moderating the timing and intensity of primary
326 production and thus biological pCO_2 drawdown.

https://doi.org/10.5194/os-2020-65
Preprint. Discussion started: 3 July 2020
© Author(s) 2020. CC BY 4.0 License.

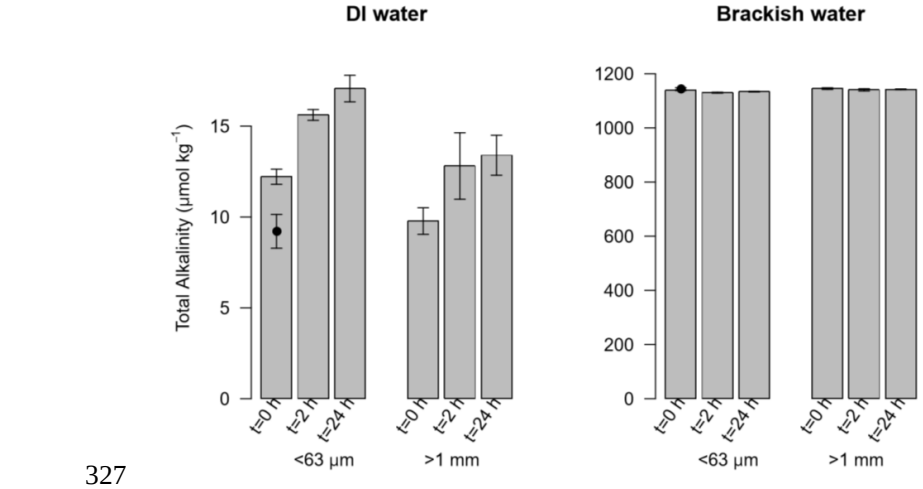

Figure 5. Total alkalinity released after leaching 4 g L^{-1} ash of two size fractions (<63 µm and >1.0 mm) in de-ionized water (DI water) and brackish water. T_0= 'time zero', measured after one minute of mixing, T_{2H}= after two hours of mixing, T_{24H}= after 24 hours of mixing. n=4 for all treatments (mean ± standard deviation plotted). The initial (pre-ash addition) alkalinity is marked by a black dot superimposed on the left T_0.

Ion Chromatography results for Na, K, Ca, Fl, Cl, NO_3 and SO_4 showed that in the presence of smaller ash size particles, ion inputs were generally higher and that the dissolution from ash components occurred almost instantly with limited, or no increases in leached concentrations observed between 0, 2 and 24 h (Table 1). For larger particles there was less release of most ions. In the case of Ca and SO_4 a more gradual leaching effect was apparent (Table 1). The concentrations of NO_3 and NH_4 and were generally below detection suggesting that ash was a minor source of these macronutrients into solution. These observations are consistent with the trends in prior work using a range of volcanic ash and incubation conditions (Delmelle et al., 2007; Duggen et al., 2010; Witham et al., 2005).

https://doi.org/10.5194/os-2020-65
Preprint. Discussion started: 3 July 2020
© Author(s) 2020. CC BY 4.0 License.

	Time (hours)	Na	K	Ca	Fl	Cl	NO_3	NH_4	SO_4
Detection limit	*n/a*	*0.10*	*0.11*	*0.16*	*0.28*	*1.31*	*0.34*	*0.19*	*1.07*
Procedural blank	*n/a*	*b.d.*	*0.36*	*0.39*	*b.d.*	*b.d.*	*b.d.*	*b.d.*	b.d.
<63 µm ash	0 (post ash)	16.23	3.15	25.06	0.29	17.08	0.53	1.70	13.47
	2	16.73	3.78	31.82	0.63	15.16	b.d.	0.52	18.97
	24	17.28	3.91	33.75	0.69	14.63	b.d.	1.32	18.82
>1.0 mm ash	0 (post ash)	b.d.	0.35	b.d.	b.d.	b.d.	b.d.	0.30	b.d.
	2	3.41	0.83	18.28	b.d.	3.71	b.d.	b.d.	3.65
	24	5.10	1.02	18.53	b.d.	4.40	b.d.	0.38	4.93

Table 1. Ion concentration in µmol l^{-1} leached from two size fractions of ash (<63 µm and >1.0 mm) into de-ionized water. b.d = below detection. The procedural blank refers to water handled as a sample but without ash addition. All values are mean (n = 4) concentrations after deduction of the procedural blank.

3.4 Trace elements in leach experiments

Release of nanomolar concentrations of dissolved Fe, Mn and Cu was evident when ash was re-suspended in aged seawater for 10 minutes (Fig. 6). The efficiency of dFe release from volcanic ash was variable with the most efficient release of dFe per unit mass of ash addition (1200 nmol g^{-1}) achieved at the lowest loading per unit volume of seawater tested (<10 mg L^{-1}). Conversely, the release of dissolved Mn and Cu increased linearly (R^2 0.99) over the

https://doi.org/10.5194/os-2020-65
Preprint. Discussion started: 3 July 2020
© Author(s) 2020. CC BY 4.0 License.

applied ash gradient (0.1 - 6 mg L^{-1}). This demonstrates that the reduced dissolution efficiency of Fe at high particle loads was related to the chemistry of dFe which is a readily scavenged element in seawater (de Baar and de Jong, 2001; Johnson et al., 1997). Dissolved Co, Pb and Ni concentrations increased with ash loading similarly to Mn and Cu, but with weaker linear relationships between metal concentration and ash loading (Fig. 6). No clear increase in dissolved Cd concentrations was evident with increased ash loading. Non-linearity between ash addition and trace metal concentrations, and negative changes in concentrations under some conditions, both likely reflect scavenging of metal ions onto ash particle surfaces (Rogan et al., 2016).

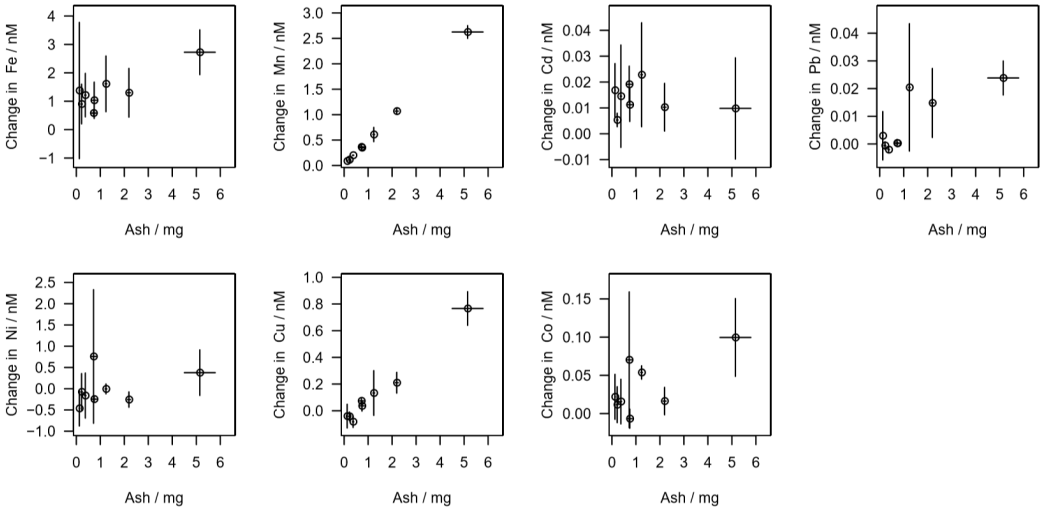

Figure 6. Change in trace metal concentrations after varying ash addition to 100 ml South Atlantic seawater for a 10 minute leach duration at room temperature. Initial (mean ± standard deviation) dissolved trace metal concentrations -deducted from the final concentrations to calculate the change as a result of ash addition- were 0.98 ± 0.03 nM Fe, 0.38 ± 0.04 nM Cd, 13 ± 2 pM Pb, 6.58 ± 0.76 nM Ni, 0.84 ± 0.07 nM Cu, 145 ± 9 pM Co, 0.72 ± 0.05 nM Mn. Error bars are standard deviations from triplicate treatments.

https://doi.org/10.5194/os-2020-65
Preprint. Discussion started: 3 July 2020
© Author(s) 2020. CC BY 4.0 License.

Ocean Science
Discussions
Open Access
EGU

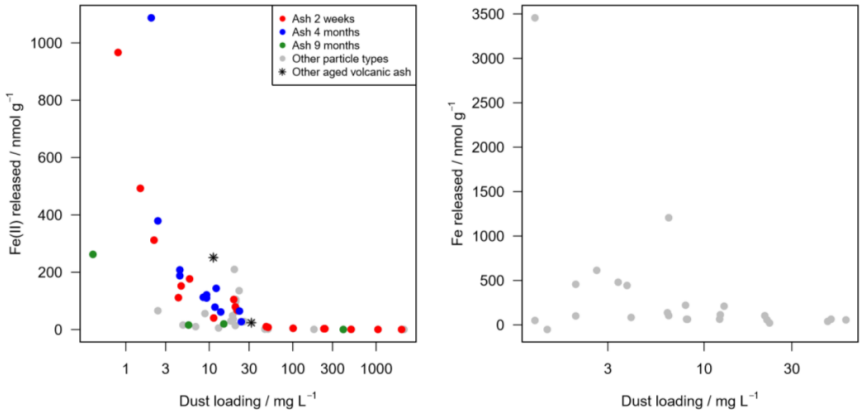

Figure 7. Fe release from ash into seawater. Mean Fe(II) released into South Atlantic seawater over a 30 minute leach at 5-7°C (left). The same batch of Calbuco ash was subsampled and used to conduct experiments on 3 occasions after the 2015 eruption (2 weeks, 4 months and 9 months since ash collection) and contrasted with other aged particles from different sources including volcanic ash retained from the 2002/2008 eruptions of Etna and Chaitén respectively (see Supplementary Table). Dissolved Fe released into South Atlantic seawater over a 10 minute leach at room temperature, data as per Fig. 6 with individual replicates shown for clarity (right).

In addition to the release of dFe in solution, which generally exists as Fe(III) species in oxic seawater (Gledhill and Buck, 2012), the release of Fe(II) was evident on a similar timescale (Fig. 7). Elevated concentrations of up to 4.0 nM Fe(II) were evident when ash was suspended in cold (5-7°C) aged S Atlantic seawater. A sharp decline in Fe(II) dissolution efficiency with increasing ash load was evident (Fig. 7). Both the highest Fe(II) concentration, and the highest net release of Fe(II), was observed at the lowest ash loading (Fig. 7). Fe(II) release was more intense for freshly collected ash particles at low ash

https://doi.org/10.5194/os-2020-65
Preprint. Discussion started: 3 July 2020
© Author(s) 2020. CC BY 4.0 License.


386 loadings, but traces of Fe(II) were found to be released from similar suspensions of other
387 particle types (Saharan dust, glacial flour, iceberg borne particles) at intermediate loadings
388 and from two other aged volcanic ash samples stored since 2002/2008 (Fig. 7).
389
390 For Calbuco volcanic ash, Fe(II) concentration following dust addition into seawater was
391 noticeably reduced when the same experimental leaches with ash were repeated 9 months
392 after the initial experiment. The first leaches were conducted ~2 weeks after ash collection.
393 The release of Fe(II) from ash therefore appeared to decrease with aging. For comparison,
394 the trace metal leach experiments (Fig. 6) were conducted at the same time as the first Fe(II)
395 incubation experiments (i.e. 2 weeks after ash collection).
396 **3.5 Satellite observations**
397 Five-day composite images of atmospheric aerosol loading (UV aerosol index) indicated two
398 main volcanic eruption plume trajectories: (i) northwards over the Pacific, and (ii) northeast
399 over the Atlantic. Daily resolved time series were constructed for regions in the Atlantic and
400 Pacific with elevated atmospheric aerosol loading (UV Aerosol Index ~2 a.u.; Fig. 8). The
401 Pacific time series indicated a pronounced peak in aerosol index followed by chlorophyll-a
402 one day later. Conversely in the Atlantic, where the background chlorophyll-a concentration
403 was higher throughout the time period of interest, the enhanced aerosol index was not clearly
404 associated with a change in chlorophyll-a dynamics (Fig. 8).

https://doi.org/10.5194/os-2020-65
Preprint. Discussion started: 3 July 2020
© Author(s) 2020. CC BY 4.0 License.

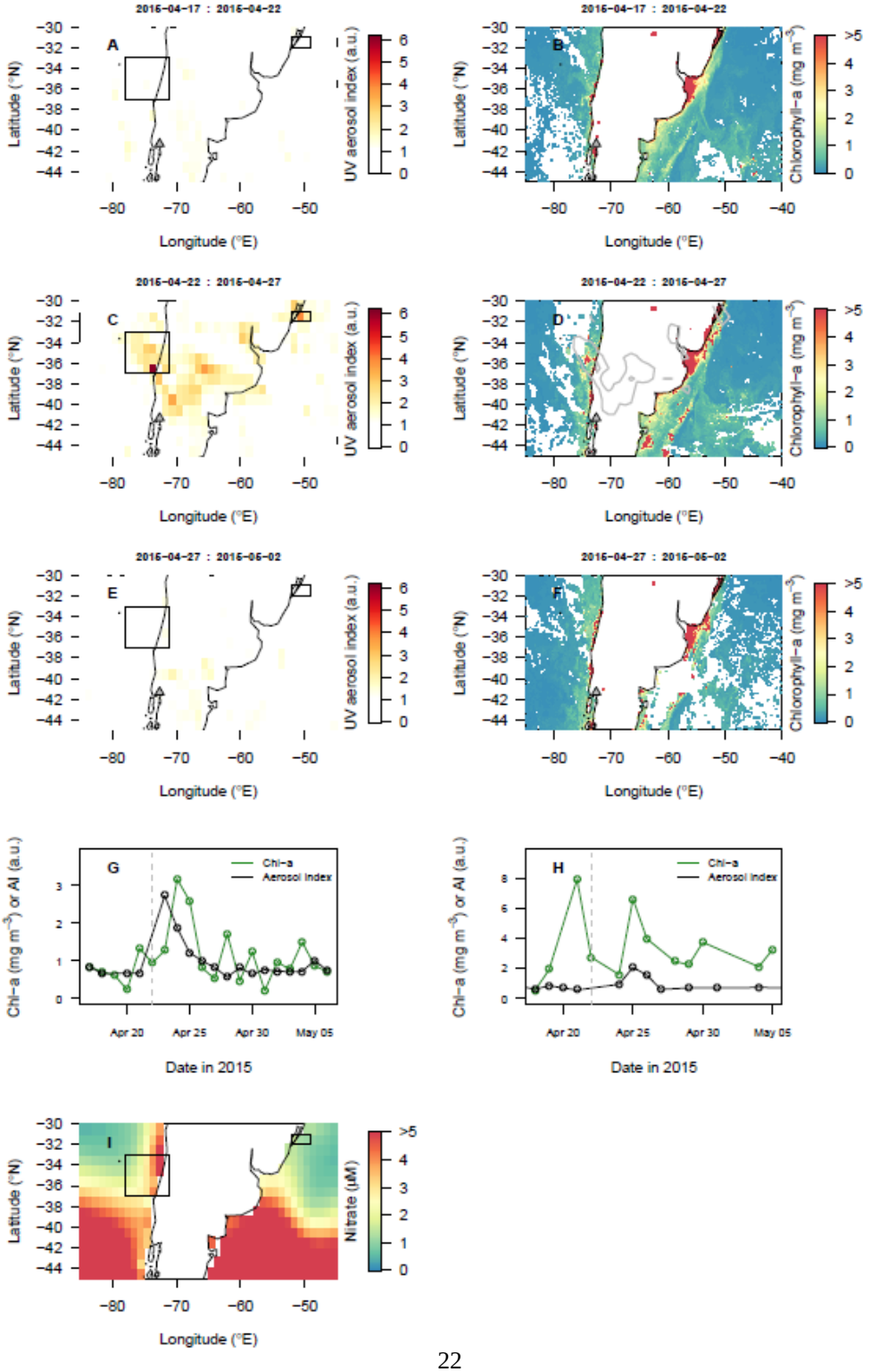

https://doi.org/10.5194/os-2020-65
Preprint. Discussion started: 3 July 2020
© Author(s) 2020. CC BY 4.0 License.


406 Figure 8. Potential biological impact of the 2015 Calbuco eruption observed via satellite
407 remote sensing. (A-F) Spatial maps showing the distribution of ash in the atmosphere (UV
408 Aerosol Index) and corresponding images of chlorophyll-a. Images were composited over 5-
409 day periods. Grey lines in chlorophyll maps corresponds to the UV Aerosol index = 2 a.u.
410 contour. (G, H) Time series of UV Aerosol Index and chlorophyll-a for regions of the Pacific
411 (G) and Atlantic (H) identified by boxes in maps. Dashed vertical lines (22 April) indicate
412 the eruption date. (I) Mean World Ocean Atlas surface NO_3 concentrations.
413
414 **4 Discussion**
415 **4.1 Local drivers of 2015 bloom dynamics in Reloncaví Fjord**
416 The north Patagonian archipelago and fjord region have a seasonal phytoplankton bloom
417 cycle with peaks in productivity occurring in May and October (austral autumn and spring)
418 and the lowest productivity consistently in June (austral winter) (González et al., 2010).
419 Diatoms normally dominate the phytoplankton community during the productive period due
420 to high light availability and high silicic acid supply, both of which are influenced by
421 freshwater runoff (González et al., 2010; Torres et al., 2014). The austral fall season,
422 encompassing the April-May 2015 ash fall, is therefore expected to have a high
423 phytoplankton biomass (Iriarte et al., 2007; León-Muñoz et al., 2018) which terminates
424 abruptly with decreasing light availability in austral winter (González et al., 2010).
425
426 Whilst not directly comparable, the magnitude of the 2015 bloom in terms of diatom
427 abundance (Fig. 4) was more intense than that reported in Reloncaví Sound 2001-2008. With
428 respect to the timing of the phytoplankton bloom, the low diatom abundances and
429 chlorophyll-a concentrations at the end of May (Fig. 4) are consistent with prior observations

https://doi.org/10.5194/os-2020-65
Preprint. Discussion started: 3 July 2020
© Author(s) 2020. CC BY 4.0 License.


of sharp declines in primary production moving into June (González et al., 2010). Peaks in diatom abundance were measured at two stations on 16 May, and measured chlorophyll-a concentrations were highest close to Station C on 30 April (Fig. 4). Station A, with the strongest freshwater influence, did not show such a pronounced peak in diatom abundance (Fig. 3). The high-resolution pH and O_2 data collected at Station C from mooring data is consistent with an intense phytoplankton bloom between ~29 April and 7 May (Fig. 3) indicated by a shift to slightly higher pH and O_2 during this time period when river flow into the fjord was stable.

Without a direct measure of ash deposition m^{-2} in the fjord, turbidity, or higher resolution chlorophyll/diatom data, it is challenging to unambiguously determine the extent to which the austral autumn phytoplankton bloom was affected by volcanic activity. The high abundance of diatoms at two of three stations sampled could have resulted from ash fertilization. Yet if this was the case, it is questionable what nutrient was responsible for this fertilization, why the bloom initiation occurred several weeks after the eruption, and to what extent the timing was coincidental given that productivity normally peaks in May. Reloncaví Fjord was to the south of the dominant ash deposition (Romero et al., 2016). Both runoff and rainfall were vectors by which ash was deposited in the fjord, which complicates the interpretation of the time series provided by high resolution data (Fig. 3). With incident light also highly variable over the time series (Fig. 3), there are clearly several factors, other than volcanic ash deposition, which will have exerted some influence on diatom and chlorophyll-a abundance throughout May 2015.

https://doi.org/10.5194/os-2020-65
Preprint. Discussion started: 3 July 2020
© Author(s) 2020. CC BY 4.0 License.


453 Primary production in the Reloncaví region is thought to be limited by light availability rather
454 than macronutrient availability (González et al., 2010). Whilst micronutrient availability
455 relative to phytoplankton demand has not been extensively assessed in this fjord, with such
456 higher riverine inputs across the region- which are normally a large source of dissolved trace
457 elements into coastal waters (e.g. Boyle et al., 1977)- limitation of phytoplankton growth by
458 Fe, or another micronutrient, seems implausible. Reported Fe concentrations determined by
459 a diffusive gel technique in Reloncaví Fjord in October 2006 were found to be relatively
460 high; 46-530 nM (Ahumada et al., 2011). Similarly, reported dFe concentrations in the
461 adjacent Comau Fjord at higher salinity are generally in the nanomolar range and remain >2
462 nM even under post-bloom conditions which suggests dFe is not a limiting factor for
463 phytoplankton growth (Hopwood et al., 2020; Sanchez et al., 2019).
464
465 Silicic acid availability could have been increased by ash deposition. Whilst not quantified
466 herein, an increase in silicic acid availability from ash in a region where silicic acid was sub-
467 optimal for diatom growth could therefore plausibly explain higher than usual diatom
468 abundance (Siringan et al., 2018). Silicic acid concentrations were indeed high (up to 80 µM)
469 in Reloncaví Fjord surface waters in May 2015 (Yevenes et al., 2019), however
470 concentrations in excess of 30 µM are typical during periods of high runoff and accordingly
471 are not thought to limit primary production or diatom growth (González et al., 2010). The
472 Si:NO_3 ratio in Reloncaví Fjord and downstream Reloncaví Sound also indicates an excess
473 of Si, with ratios of approximately 2:1 observed in fjord surface waters throughout the year
474 (González et al., 2010; Yevenes et al., 2019). For comparison, the ratio of Si:N for diatom
475 nutrient uptake is 15:16 (Brzezinski, 1985). Furthermore, experimental incubations making
476 additions of macronutrients to fjord waters in Reloncaví and adjacent fjords, have found

https://doi.org/10.5194/os-2020-65
Preprint. Discussion started: 3 July 2020
© Author(s) 2020. CC BY 4.0 License.


477 strong responses of phytoplankton to additions of Si only when Si and NO_3 were added in
478 combination, further corroborating the hypothesis that an excess of Si is normally present in
479 surface waters of these fjord systems (Labbé-Ibáñez et al., 2015). It is therefore doubtful that
480 changes in nutrient availability from ash alone could explain such high diatom abundances
481 in mid-May.
482
483 Alternative reasons for high diatom abundances in the absence of a chemical fertilization
484 effect are plausible and could include, for example, ash having reduced zooplankton
485 abundance or virus activity in the fjord, thus facilitating higher diatom abundance than would
486 otherwise have been observed by decreasing diatom mortality rates in an environment where
487 nutrients were replete. The role of volcanic ash in driving such short-term ecological shifts
488 in the marine environment is almost entirely unstudied (Weinbauer et al., 2017). However,
489 volcanic ash deposition of +7 mg L^{-1} in lakes within this region during the 2011 Puyehue-
490 Cordón Caulle eruption was reported to increase post-deposition phytoplankton biomass and
491 decrease copepod and cladoceran biomass (Wolinski et al., 2013). The proposed mechanism
492 was ash particle ingestion negatively affecting zooplankton and ash-shading positively
493 affecting phytoplankton via reduced photoinhibition (Balseiro et al., 2014; Wolinski et al.,
494 2013).
495
496 Considering the more modest peak in diatom abundance at the most strongly ash affected
497 station (Station A, Fig. 4) and the timing of the peak diatom abundance 3 weeks after the
498 eruption, it is clear that the interaction between ash and phytoplankton in the Reloncaví Fjord
499 was more complex than the simple Fe-fertilization proposed for the SE Pacific (Fig. 8g). In
500 the absence of an immediate diatom fertilization effect from Fe or silicic acid, we hypothesize

https://doi.org/10.5194/os-2020-65
Preprint. Discussion started: 3 July 2020
© Author(s) 2020. CC BY 4.0 License.


that any change in phytoplankton bloom dynamics within Reloncaví Fjord was mainly a 'top-down' effect driven by the physical interaction of ash and different ecological groups in a nutrient replete environment, rather than a 'bottom-up' effect driven by alleviation of nutrient-limitation from ash dissolution.

4.2 Volcanic ash as a unique source of trace elements

The release of the bioessential elements Fe and Mn from ash here ranged from 53 - 1200 nmol g^{-1} (dFe) and 48 - 71 nmol g^{-1} (dissolved Mn), which is comparable to the rates determined in other studies under similar experimental conditions (Duggen et al., 2010), although the dFe released at the lowest ash loading is at the high end of reported values (Fig. 6). Neither Fe(II) or dFe release increased linearly with ash loading, with the Fe(II) release particularly efficient at ash loadings <5 mg L^{-1} (Fig. 7). Unlike dissolved Cu and Mn, a more efficient release of dFe at low ash loading highlights the dual role of ash particles as both a source of dFe and also a large surface area onto which metal ions can be scavenged (Rogan et al., 2016).

Fe(II) is short lived in surface seawater with an observed half-life of only 10-20 minutes even in the cold surface waters of the Southern Ocean which slow Fe(II) oxidation (Sarthou et al., 2011). Yet, relative to Fe(III), Fe(II) is also more soluble and, from an energetic perspective, expected to be more bioaccessible to cellular uptake (Sunda et al., 2001). Fe(II) salts are expected to be present on the surface of ash particles (Horwell et al., 2003; Hoshyaripour et al., 2015) and thus Fe(II) may be released into seawater almost instantaneously when fresh deposition of volcanic ash occurs following dissolution of thin layers of salt coatings in ash surfaces (Ayris and Delmelle, 2012; Delmelle et al., 2007). Upon aging of dry ash, the Fe(II) concentration leached from ash decreased sharply between 4 and 9 months after the eruption,

https://doi.org/10.5194/os-2020-65
Preprint. Discussion started: 3 July 2020
© Author(s) 2020. CC BY 4.0 License.


suggesting an on-going conversion of Fe(II) to Fe(III) on ash particle surfaces (Fig. 7). The precise cause of this is uncertain from our experiments, yet we can speculate that as Fe(II) on fresh ash surfaces is expected to be associated with acidic surface coatings, it could be a 'self-neutralization' effect where the low surface pH of Fe(II)-rich zones is slowly neutralized by interaction with the more alkaline bulk material. Irrespective of the underlying cause, this implies that the bioavailability of Fe within freshly deposited ash would be higher than aged ash, or other un-processed aerosols. Standard leaching protocols are thereby unlikely to resolve the release of Fe(II) that could occur under environmentally relevant conditions. Different leaching protocols are widely recognised as a major challenge for interpreting and comparing different dissolution experiment datasets for all types of aerosols (Duggen et al., 2010; Morton et al., 2013). In any case, a decline in the release of dFe from volcanic ash upon aging under the same storage conditions (bulk dry samples) has been noted previously (Duggen et al., 2010), but was thought to be a slow process with a time period of 10-20 years required for the dFe leached within an hour in seawater to fall by half (Olgun et al., 2011). The much more rapid 50-90% decline in the Fe(II) released into seawater occurring between 2 weeks and 9 months after the eruption likely reflects much faster changes in the surface composition of ash which may not be evident in leaches conducted under conditions unfavourable for Fe(II) release (e.g. at room temperature), or when baseline experimental leaches for evaluating aging effects are conducted several months after the collection of ash.

The dFe and Fe(II) leaching protocols used herein are not directly comparable, as the Fe(II) method using cooler seawater and larger seawater volumes was specifically designed to test for the presence of rapid Fe(II) release. Yet, for rough comparative purposes, the Fe(II)

https://doi.org/10.5194/os-2020-65
Preprint. Discussion started: 3 July 2020
© Author(s) 2020. CC BY 4.0 License.


549 released was equivalent to 38 ± 25% (mean ± standard deviation) of dFe released at ash
550 loadings from 1-10 mg L^{-1} and 19 ± 17% of dFe for ash loadings from 10-50 mg L^{-1}. These
551 values are reasonably comparable to the 26% median Fe(II)/dFe fraction measured in Fe
552 released into seawater from aerosols collected over the Pacific Ocean (Buck et al., 2013)
553 suggesting that fresh volcanic ash is roughly comparable in terms of Fe(II) lability to these
554 aerosols.

555 **4.3 A potential fertilization effect in the SE Pacific**

556 Experiments with ash suspensions have shown that ash loading has a restricted impact on
557 satellite chlorophyll-a retrieval (Browning et al., 2015), therefore offering a means to assess
558 the potential biological impact of the 2015 Calbuco eruption in offshore waters. We found
559 evidence for fertilization of offshore Pacific seawaters (Fig. 8). Following the eruption date,
560 mean chlorophyll-a concentrations increased ~2.5 times over a broad region where elevated
561 atmospheric aerosol loading was detected (Fig. 8G). Both the timing and location of this
562 chlorophyll-a peak were consistent with ash fertilization, with the peak of elevated
563 chlorophyll-a being located within the core of highest atmospheric aerosol loading, and the
564 peak date occurring one day after the main passage of the atmospheric aerosol plume. A
565 similar phytoplankton response timeframe was reported following ash deposition in the NE
566 Pacific following the August 2008 Kasatochi eruption (Hamme et al., 2010) which was
567 similarly thought to be triggered by relief of Fe-limitation (Langmann et al., 2010).

568

569 The change in chlorophyll-a observed in the SE Pacific contrasts with results in Reloncaví
570 Fjord where phytoplankton abundances were lowest at the strongest ash-influenced station
571 (Station A, Fig.1) and likely peaked much later than the first ash arrival- after 28 April. The
572 fertilized region of the Pacific (Fig. 8) hosts upwelling of deep waters, supplying nutrients in

https://doi.org/10.5194/os-2020-65
Preprint. Discussion started: 3 July 2020
© Author(s) 2020. CC BY 4.0 License.


573 ratios that are deficient in dFe (Bonnet et al., 2008; Torres and Ampuero, 2009). Fe-limitation
574 of phytoplankton growth in this region is therefore anticipated, which could have been
575 temporarily relieved following ash deposition and dFe release (Fig. 6). Conversely, ash
576 deposition into the south western Atlantic indicated by atmospheric aerosol loading did not
577 lead to any clear corresponding change in chlorophyll-a concentrations (Fig. 8H).
578 Phytoplankton growth in this region of the Atlantic is expected to be limited by fixed nitrogen
579 availability, as a result of strong stratification (Moore et al., 2013) and thus dFe release from
580 ash particles would not be expected to result in short-term increases to primary production.
581 The differential responses observed in the Pacific and Atlantic are therefore consistent with
582 the anticipated nutrient limitation regimes (Fe-limited and nitrogen-limited, respectively),
583 and the supply of dFe but not fixed N (NO_3 or NH_4) from the Calbuco ash (Fig. 6 and Table
584 1).
585
586 **5 Conclusions**
587 The contrasting effects of volcanic ash on primary producers in Reloncaví Fjord, the SE
588 Pacific and SW Atlantic support the hypothesis that the response of primary producers is
589 highly dependent on both the ash loading and the resources limiting primary production in a
590 region at a specific time of year. Leach experiments using ash from the 2015 Calbuco
591 eruption demonstrated a small increase in the alkalinity of de-ionized water from fine, but
592 not coarse ash, and no significant addition of fixed nitrogen (quantified as NO_3 and NH_4) into
593 solution. In saline waters, release of dissolved trace metals including Mn, Cu, Ni, Co, Pb, Fe
594 and specifically Fe(II) was evident.
595

https://doi.org/10.5194/os-2020-65
Preprint. Discussion started: 3 July 2020
© Author(s) 2020. CC BY 4.0 License.


596 Strong evidence of a broad-scale 'bottom-up' fertilization effect of ash on primary production
597 was not found locally within Reloncaví Fjord, although the timing and peak diatom
598 abundance of the autumn phytoplankton bloom may have shifted in response to high ash
599 loading in the weeks following the eruption. High diatom abundances at some stations within
600 the fjord several weeks after the eruption may have arisen from a 'top-down' effect of ash on
601 filter feeders, although the mechanism can only be speculated herein. No clear positive effect
602 of ash deposition on chlorophyll-a was evident in the SW Atlantic, consistent with expected
603 patterns in nutrient deficiency which suggest the region to be nitrogen-limited. However, in
604 offshore waters of the SE Pacific where Fe is anticipated to limit phytoplankton growth, a
605 close correlation between maximum ash deposition and an increase in chlorophyll-a was
606 likely driven by Fe-fertilization.
607

608 **6. Data availability**

609 The complete 2015 time series from the Reloncaví Fjord mooring is available online
610 (https://figshare.com/articles/Puelo_Bouy/7754258). Source data for Figures 4-7 is included
611 in the Supplement.
612

613 **7. Acknowledgements**

614 The authors thank the Dirección de Investigación & Desarrollo UACh for its partial support
615 during this project. The data presented are part of the second chapter of the PhD Thesis of
616 MVJ at Universidad Austral de Chile. Cristian Vargas (Universidad de Concepción) is
617 thanked for making additional chlorophyll a data available, Manuel Díaz for providing Fig.
618 1 and Miriam Beck for assistance with Fe(II) flow injection analysis.
619

https://doi.org/10.5194/os-2020-65
Preprint. Discussion started: 3 July 2020
© Author(s) 2020. CC BY 4.0 License.


8. Funding

JLI and EA gratefully acknowledge funding from the European Commission (OCEAN-CERTAIN, FP7- ENV- 2013-6.1-1; no: 603773). JLI received funding by CONICYT-FONDECYT 1141065 and is partially funded by Center IDEAL (FONDAP 15150003). Partial funding came from CONICYT-FONDECYT 1140385 (RT). MVJ received financial support from a CONICYT Scholarship (Beca Doctorado Nacional 2015 No 21150285). IR and MH received funding from the Deutsche Forschungsgemeinschaft as part of Sonderforschungsbereich (SFB) 754: 'Climate-Biogeochemistry Interactions in the Tropical Ocean'.

9. Author contributions

MVJ, MH, JLI and EA designed the study. MVJ, IR, MH, RT and BR conducted analytical and field work. TB conducted satellite data analysis. MV, MH and TB wrote the initial manuscript with all authors contributing to its revision.

10. References

Achterberg, E. P., Moore, C. M., Henson, S. A., Steigenberger, S., Stohl, A., Eckhardt, S., Avendano, L. C., Cassidy, M., Hembury, D., Klar, J. K., Lucas, M. I., Macey, A. I., Marsay, C. M. and Ryan-Keogh, T. J.: Natural iron fertilization by the Eyjafjallajokull volcanic eruption, Geophys. Res. Lett., 40(5), 921–926, doi:10.1002/grl.50221, 2013.

Ahumada, R., Rudolph, A., Gonzalez, E., Fones, G., Saldias, G. and Ahumada Rudolph, R.: Dissolved trace metals in the water column of Reloncavi Fjord, Chile, Lat. Am. J. Aquat. Res., 39, 567–574, doi:10.3856/vol39-issue3-fulltext-16, 2011.

https://doi.org/10.5194/os-2020-65
Preprint. Discussion started: 3 July 2020
© Author(s) 2020. CC BY 4.0 License.


644 Ayris, P. and Delmelle, P.: Volcanic and atmospheric controls on ash iron solubility: A
645 review, Phys. Chem. Earth, doi:10.1016/j.pce.2011.04.013, 2012.
646 de Baar, H. J. W. and de Jong, J. T. M.: Distributions, sources and sinks of iron in seawater,
647 in The Biogeochemistry of Iron in Seawater. IUPAC Series on Analytical and Physical
648 Chemistry of Environmental Systems, pp. 123–253., 2001.
649 Balseiro, E., Souza, M. S., Olabuenaga, I. S., Wolinski, L., Navarro, M. B.,
650 Laspoumaderes, C. and Modenutti, B.: Effect of the Puyehue-Cordon Caulle volcanic
651 complex eruption on crustacean zooplankton of Andean Lakes, Ecol. Austral, 2014.
652 Bonnet, S., Guieu, C., Bruyant, F., Prášil, O., Van Wambeke, F., Raimbault, P., Moutin, T.,
653 Grob, C., Gorbunov, M. Y., Zehr, J. P., Masquelier, S. M., Garczarek, L. and Claustre, H.:
654 Nutrient limitation of primary productivity in the Southeast Pacific (BIOSOPE cruise),
655 Biogeosciences, 5(1), 215–225, doi:10.5194/bg-5-215-2008, 2008.
656 Boyle, E. A., Edmond, J. M. and Sholkovitz, E. R.: Mechanism of iron removal in
657 estuaries, Geochim. Cosmochim. Acta, 41(9), 1313–1324, doi:10.1016/0016-
658 7037(77)90075-8, 1977.
659 Browning, T. J., Bouman, H. A., Henderson, G. M., Mather, T. A., Pyle, D. M., Schlosser,
660 C., Woodward, E. M. S. and Moore, C. M.: Strong responses of Southern Ocean
661 phytoplankton communities to volcanic ash, Geophys. Res. Lett., 41(8), 2851–2857,
662 doi:10.1002/2014GL059364, 2014.
663 Browning, T. J., Stone, K., Bouman, H., Mather, T. A., Pyle, D. M., Moore, M. and
664 Martinez-Vicente, V.: Volcanic ash supply to the surface ocean – remote sensing of
665 biological responses and their wider biogeochemical significance, Front. Mar. Sci., 2,
666 doi:10.3389/fmars.2015.00014, 2015.
667 Brzezinski, M. A.: The Si:C:N ratio of marine diatoms: interspecific variability and the

https://doi.org/10.5194/os-2020-65
Preprint. Discussion started: 3 July 2020
© Author(s) 2020. CC BY 4.0 License.


668 effect of some environmental variables, J. Phycol., 21(3), 347–357, doi:10.1111/j.0022-
669 3646.1985.00347.x, 1985.
670 Buck, C. S., Landing, W. M. and Resing, J.: Pacific Ocean aerosols: Deposition and
671 solubility of iron, aluminum, and other trace elements, Mar. Chem., 157, 117–130,
672 doi:10.1016/j.marchem.2013.09.005, 2013.
673 Castillo, M. I., Cifuentes, U., Pizarro, O., Djurfeldt, L. and Caceres, M.: Seasonal
674 hydrography and surface outflow in a fjord with a deep sill: The Reloncaví fjord, Chile,
675 Ocean Sci., 12, 533–544, doi:10.5194/os-12-533-2016, 2016.
676 DeGrandpre, M. D., Hammar, T. R., Smith, S. P. and Sayles, F. L.: In situ measurements of
677 seawater pCO2, Limnol. Oceanogr., 40(5), 969–975, doi:10.4319/lo.1995.40.5.0969, 1995.
678 DeGrandpre, M. D., Baehr, M. M. and Hammar, T. R.: Calibration-free optical chemical
679 sensors, Anal. Chem., 71(6), 1152–1159, doi:10.1021/ac9805955, 1999.
680 Delmelle, P., Lambert, M., Dufrêne, Y., Gerin, P. and Óskarsson, N.: Gas/aerosol-ash
681 interaction in volcanic plumes: New insights from surface analyses of fine ash particles,
682 Earth Planet. Sci. Lett., 259, 159–170, doi:10.1016/j.epsl.2007.04.052, 2007.
683 Duggen, S., Olgun, N., Croot, P., Hoffmann, L., Dietze, H., Delmelle, P. and Teschner, C.:
684 The role of airborne volcanic ash for the surface ocean biogeochemical iron-cycle: a
685 review, Biogeosciences, 7(3), 827–844, doi:10.5194/bg-7-827-2010, 2010.
686 Van Eaton, A. R., Amigo, Á., Bertin, D., Mastin, L. G., Giacosa, R. E., González, J.,
687 Valderrama, O., Fontijn, K. and Behnke, S. A.: Volcanic lightning and plume behavior
688 reveal evolving hazards during the April 2015 eruption of Calbuco volcano, Chile,
689 Geophys. Res. Lett., 43(7), 3563–3571, doi:10.1002/2016GL068076, 2016.
690 Ermolin, M. S., Fedotov, P. S., Malik, N. A. and Karandashev, V. K.: Nanoparticles of
691 volcanic ash as a carrier for toxic elements on the global scale, Chemosphere, 200, 16–22,

https://doi.org/10.5194/os-2020-65
Preprint. Discussion started: 3 July 2020
© Author(s) 2020. CC BY 4.0 License.


692 doi:10.1016/j.chemosphere.2018.02.089, 2018.
693 Frogner, P., Gislason, S. R. and Oskarsson, N.: Fertilizing potential of volcanic ash in
694 ocean surface water, Geology, 29(6), 487–490, doi:10.1130/0091-
695 7613(2001)029<0487:fpovai>2.0.co;2, 2001.
696 Gledhill, M. and Buck, K. N.: The organic complexation of iron in the marine environment:
697 a review, Front. Microbiol., 3, 69, doi:10.3389/fmicb.2012.00069, 2012.
698 González, H. E., Calderón, M. J., Castro, L., Clement, A., Cuevas, L. A., Daneri, G., Iriarte,
699 J. L., Lizárraga, L., Martínez, R., Menschel, E., Silva, N., Carrasco, C., Valenzuela, C.,
700 Vargas, C. A. and Molinet, C.: Primary production and plankton dynamics in the Reloncaví
701 Fjord and the Interior Sea of Chiloé, Northern Patagonia, Chile, Mar. Ecol. Prog. Ser., 402,
702 13–30, 2010.
703 Hamme, R. C., Webley, P. W., Crawford, W. R., Whitney, F. A., Degrandpre, M. D.,
704 Emerson, S. R., Eriksen, C. C., Giesbrecht, K. E., Gower, J. F. R., Kavanaugh, M. T., Pea,
705 M. A., Sabine, C. L., Batten, S. D., Coogan, L. A., Grundle, D. S. and Lockwood, D.:
706 Volcanic ash fuels anomalous plankton bloom in subarctic northeast Pacific, Geophys. Res.
707 Lett., 37(19), L19604, doi:10.1029/2010GL044629, 2010.
708 Haraldsson, C., Anderson, L. G., Hassellöv, M., Hulth, S. and Olsson, K.: Rapid, high-
709 precision potentiometric titration of alkalinity in ocean and sediment pore waters, Deep Sea
710 Res. Part I Oceanogr. Res. Pap., 44(12), 2031–2044, doi:10.1016/S0967-0637(97)00088-5,
711 1997.
712 Hoffmann, L. J., Breitbarth, E., Ardelan, M. V., Duggen, S., Olgun, N., Hassellöv, M. and
713 Wängberg, S.-Å.: Influence of trace metal release from volcanic ash on growth of
714 Thalassiosira pseudonana and Emiliania huxleyi, Mar. Chem., 132–133, 28–33,
715 doi:10.1016/j.marchem.2012.02.003, 2012.

https://doi.org/10.5194/os-2020-65
Preprint. Discussion started: 3 July 2020
© Author(s) 2020. CC BY 4.0 License.


716 Hopwood, M. J., Santana-González, C., Gallego-Urrea, J., Sanchez, N., Achterberg, E. P.,
717 Ardelan, M. V., Gledhill, M., González-Dávila, M., Hoffmann, L., Leiknes, Ø., Magdalena
718 Santana-Casiano, J., Tsagaraki, T. M. and Turner, D.: Fe(II) stability in coastal seawater
719 during experiments in Patagonia, Svalbard, and Gran Canaria, Biogeosciences,
720 doi:10.5194/bg-17-1327-2020, 2020.
721 Horwell, C. J., Fenoglio, I., Vala Ragnarsdottir, K., Sparks, R. S. J. and Fubini, B.: Surface
722 reactivity of volcanic ash from the eruption of Soufrière Hills volcano, Montserrat, West
723 Indies with implications for health hazards, Environ. Res., 93(2), 202–215,
724 doi:10.1016/S0013-9351(03)00044-6, 2003.
725 Hoshyaripour, G. A., Hort, M. and Langmann, B.: Ash iron mobilization through
726 physicochemical processing in volcanic eruption plumes: A numerical modeling approach,
727 Atmos. Chem. Phys., 15, 9361–9379, doi:10.5194/acp-15-9361-2015, 2015.
728 Hu, C., Lee, Z. and Franz, B.: Chlorophyll aalgorithms for oligotrophic oceans: A novel
729 approach based on three-band reflectance difference, J. Geophys. Res. Ocean., 117(C1),
730 doi:10.1029/2011JC007395, 2012.
731 Iriarte, J. L., González, H. E., Liu, K. K., Rivas, C. and Valenzuela, C.: Spatial and
732 temporal variability of chlorophyll and primary productivity in surface waters of southern
733 Chile (41.5–43° S), Estuar. Coast. Shelf Sci., 74(3), 471–480,
734 doi:10.1016/j.ecss.2007.05.015, 2007.
735 Johnson, K. S., Gordon, R. M. and Coale, K. H.: What controls dissolved iron in the world
736 ocean?, Mar. Chem., 57, 137–161, doi:10.1016/s0304-4203(97)00043-1, 1997.
737 Jones, M. R., Nightingale, P. D., Turner, S. M. and Liss, P. S.: Adaptation of a load-inject
738 valve for a flow injection chemiluminescence system enabling dual-reagent injection
739 enhances understanding of environmental Fenton chemistry, Anal. Chim. Acta, 796, 55–60,

https://doi.org/10.5194/os-2020-65
Preprint. Discussion started: 3 July 2020
© Author(s) 2020. CC BY 4.0 License.


740 doi:10.1016/j.aca.2013.08.003, 2013.
741 Jones, M. T. and Gislason, S. R.: Rapid releases of metal salts and nutrients following the
742 deposition of volcanic ash into aqueous environments, Geochim. Cosmochim. Acta, 72(15),
743 3661–3680, doi:10.1016/j.gca.2008.05.030, 2008.
744 Labbé-Ibáñez, P., Iriarte, J. L. and Pantoja, S.: Respuesta del microfitoplancton a la adición
745 de nitrato y ácido silícico en fiordos de la Patagonia chilena, Lat. Am. J. Aquat. Res., 43(1),
746 80–93, doi:10.3856/vol43-issue1-fulltext-8, 2015.
747 Langmann, B., Zakšek, K., Hort, M. and Duggen, S.: Volcanic ash as fertiliser for the
748 surface ocean, Atmos. Chem. Phys., 10, 3891–3899, doi:10.5194/acp-10-3891-2010, 2010.
749 León-Muñoz, J., Marcé, R. and Iriarte, J. L.: Influence of hydrological regime of an Andean
750 river on salinity, temperature and oxygen in a Patagonia fjord, Chile, New Zeal. J. Mar.
751 Freshw. Res., 47(4), 515–528, doi:10.1080/00288330.2013.802700, 2013.
752 León-Muñoz, J., Urbina, M. A., Garreaud, R. and Iriarte, J. L.: Hydroclimatic conditions
753 trigger record harmful algal bloom in western Patagonia (summer 2016), Sci. Rep., 8(1),
754 1330, doi:10.1038/s41598-018-19461-4, 2018.
755 Lin, I. I., Hu, C., Li, Y. H., Ho, T. Y., Fischer, T. P., Wong, G. T. F., Wu, J., Huang, C. W.,
756 Chu, D. A., Ko, D. S. and Chen, J. P.: Fertilization potential of volcanic dust in the low-
757 nutrient low-chlorophyll western North Pacific subtropical gyre: Satellite evidence and
758 laboratory study, Global Biogeochem. Cycles, 25, GB1006, doi:10.1029/2009GB003758,
759 2011.
760 López-Escobar, L., Parada, M. A., Hickey-Vargas, R., Frey, F. A., Kempton, P. D. and
761 Moreno, H.: Calbuco Volcano and minor eruptive centers distributed along the Liquiñe-
762 Ofqui Fault Zone, Chile (41°–42° S): contrasting origin of andesitic and basaltic magma in
763 the Southern Volcanic Zone of the Andes, Contrib. to Mineral. Petrol., 119(4), 345–361,

https://doi.org/10.5194/os-2020-65
Preprint. Discussion started: 3 July 2020
© Author(s) 2020. CC BY 4.0 License.


764 doi:10.1007/BF00286934, 1995.

765 Martin, J. H., Fitzwater, S. E. and Gordon, R. M.: Iron deficiency limits phytoplankton

766 growth in Antarctic waters, Global Biogeochem. Cycles, 4(1), 5–12, 1990.

767 Mélançon, J., Levasseur, M., Lizotte, M., Delmelle, P., Cullen, J., Hamme, R. C., Peña, A.,

768 Simpson, K. G., Scarratt, M., Tremblay, J. É., Zhou, J., Johnson, K., Sutherland, N.,

769 Arychuk, M., Nemcek, N. and Robert, M.: Early response of the northeast subarctic Pacific

770 plankton assemblage to volcanic ash fertilization, Limnol. Oceanogr., 59,

771 doi:10.4319/lo.2014.59.1.0055, 2014.

772 Molinet, C., Díaz, M., Marín, S. L., Astorga, M. P., Ojeda, M., Cares, L. and Asencio, E.:

773 Relation of mussel spatfall on natural and artificial substrates: Analysis of ecological

774 implications ensuring long-term success and sustainability for mussel farming,

775 Aquaculture, 467, 211–218, doi:10.1016/j.aquaculture.2016.09.019, 2017.

776 Moore, C. M., Mills, M. M., Arrigo, K. R., Berman-Frank, I., Bopp, L., Boyd, P. W.,

777 Galbraith, E. D., Geider, R. J., Guieu, C., Jaccard, S. L., Jickells, T. D., La Roche, J.,

778 Lenton, T. M., Mahowald, N. M., Maranon, E., Marinov, I., Moore, J. K., Nakatsuka, T.,

779 Oschlies, A., Saito, M. A., Thingstad, T. F., Tsuda, A. and Ulloa, O.: Processes and

780 patterns of oceanic nutrient limitation, Nat. Geosci, 6(9), 701–710, doi:10.1038/ngeo1765,

781 2013.

782 Morton, P. L., Landing, W. M., Hsu, S. C., Milne, A., Aguilar-Islas, A. M., Baker, A. R.,

783 Bowie, A. R., Buck, C. S., Gao, Y., Gichuki, S., Hastings, M. G., Hatta, M., Johansen, A.

784 M., Losno, R., Mead, C., Patey, M. D., Swarr, G., Vandermark, A. and Zamora, L. M.:

785 Methods for the sampling and analysis of marine aerosols: Results from the 2008

786 GEOTRACES aerosol intercalibration experiment, Limnol. Oceanogr. Methods, 11,

787 doi:10.4319/lom.2013.11.62, 2013.

https://doi.org/10.5194/os-2020-65
Preprint. Discussion started: 3 July 2020
© Author(s) 2020. CC BY 4.0 License.


788 Mosley, L. M., Husheer, S. L. G. and Hunter, K. A.: Spectrophotometric pH measurement
789 in estuaries using thymol blue and m-cresol purple, Mar. Chem., 91, 175–186,
790 doi:10.1016/j.marchem.2004.06.008, 2004.
791 Newcomb, T. W. and Flagg, T. A.: Some effects of Mt. St. Helens volcanic ash on juvenile
792 salmon smolts., Mar. Fish. Rev., 45(2), 8–12, 1983.
793 Olgun, N., Duggen, S., Croot, P. L., Delmelle, P., Dietze, H., Schacht, U., Óskarsson, N.,
794 Siebe, C., Auer, A. and Garbe-Schönberg, D.: Surface ocean iron fertilization: The role of
795 airborne volcanic ash from subduction zone and hot spot volcanoes and related iron fluxes
796 into the Pacific Ocean, Global Biogeochem. Cycles, 25(4), doi:10.1029/2009GB003761,
797 2011.
798 Rapp, I., Schlosser, C., Rusiecka, D., Gledhill, M. and Achterberg, E. P.: Automated
799 preconcentration of Fe, Zn, Cu, Ni, Cd, Pb, Co, and Mn in seawater with analysis using
800 high-resolution sector field inductively-coupled plasma mass spectrometry, Anal. Chim.
801 Acta, 976, 1–13, 2017.
802 Rogan, N., Achterberg, E. P., Le Moigne, F. A. C., Marsay, C. M., Tagliabue, A. and
803 Williams, R. G.: Volcanic ash as an oceanic iron source and sink, Geophys. Res. Lett.,
804 43(6), 2732–2740, doi:10.1002/2016GL067905, 2016.
805 Romero, J. E., Morgavi, D., Arzilli, F., Daga, R., Caselli, A., Reckziegel, F., Viramonte, J.,
806 Díaz-Alvarado, J., Polacci, M., Burton, M. and Perugini, D.: Eruption dynamics of the 22–
807 23 April 2015 Calbuco Volcano (Southern Chile): Analyses of tephra fall deposits, J.
808 Volcanol. Geotherm. Res., 317, 15–29, doi:10.1016/j.jvolgeores.2016.02.027, 2016.
809 Sanchez, N., Bizsel, N., Iriarte, J. L., Olsen, L. M. and Ardelan, M. V.: Iron cycling in a
810 mesocosm experiment in a north Patagonian fjord: Potential effect of ammonium addition
811 by salmon aquaculture, Estuar. Coast. Shelf Sci., 220, 209–219,

https://doi.org/10.5194/os-2020-65
Preprint. Discussion started: 3 July 2020
© Author(s) 2020. CC BY 4.0 License.


812 doi:10.1016/j.ecss.2019.02.044, 2019.

813 Sarmiento, J. L.: Atmospheric CO2 stalled, Nature, doi:10.1038/365697a0, 1993.

814 Sarthou, G., Bucciarelli, E., Chever, F., Hansard, S. P., Gonzalez-Davila, M., Santana-

815 Casiano, J. M., Planchon, F. and Speich, S.: Labile Fe(II) concentrations in the Atlantic

816 sector of the Southern Ocean along a transect from the subtropical domain to the Weddell

817 Sea Gyre, Biogeosciences, 8(9), 2461–2479, doi:10.5194/bg-8-2461-2011, 2011.

818 Seidel, M. P., DeGrandpre, M. D. and Dickson, A. G.: A sensor for in situ indicator-based

819 measurements of seawater pH, Mar. Chem., 109(1), 18–28,

820 doi:10.1016/j.marchem.2007.11.013, 2008.

821 Siringan, F. P., Racasa, E. D. R., David, C. P. C. and Saban, R. C.: Increase in Dissolved

822 Silica of Rivers Due to a Volcanic Eruption in an Estuarine Bay (Sorsogon Bay,

823 Philippines), Estuaries and Coasts, 41, 2277–2288, doi:10.1007/s12237-018-0428-1, 2018.

824 Stewart, C., Johnston, D. M., Leonard, G. S., Horwell, C. J., Thordarson, T. and Cronin, S.

825 J.: Contamination of water supplies by volcanic ashfall: A literature review and simple

826 impact modelling, J. Volcanol. Geotherm. Res., 158(3), 296–306,

827 doi:10.1016/j.jvolgeores.2006.07.002, 2006.

828 Sunda, W. G., Buffle, J. and Van Leeuwen, H. P.: Bioavailability and Bioaccumulation of

829 Iron in the Sea, in The Biogeochemistry of Iron in Seawater, vol. 7, edited by D. R. Turner

830 and K. A. Hunter, pp. 41–84, John Wiley & Sons, Ltd, Chichester., 2001.

831 Torres, R. and Ampuero, P.: Strong CO2 outgassing from high nutrient low chlorophyll

832 coastal waters off central Chile (30°S): The role of dissolved iron, Estuar. Coast. Shelf Sci.,

833 83(2), 126–132, doi:10.1016/j.ecss.2009.02.030, 2009.

834 Torres, R., Silva, N., Reid, B. and Frangopulos, M.: Silicic acid enrichment of subantarctic

835 surface water from continental inputs along the Patagonian archipelago interior sea (41-

https://doi.org/10.5194/os-2020-65
Preprint. Discussion started: 3 July 2020
© Author(s) 2020. CC BY 4.0 License.


836 56°S), Prog. Oceanogr., 129, 50–61, doi:10.1016/j.pocean.2014.09.008, 2014.
837 Utermöhl, H.: Zur Vervollkommnung der quantitativen Phytoplankton-Methodik, SIL
838 Commun. 1953-1996, doi:10.1080/05384680.1958.11904091, 1958.
839 Vergara-Jara, M. J., DeGrandpre, M. D., Torres, R., Beatty, C. M., Cuevas, L. A., Alarcón,
840 E. and Iriarte, J. L.: Seasonal Changes in Carbonate Saturation State and Air-Sea CO2
841 Fluxes During an Annual Cycle in a Stratified-Temperate Fjord (Reloncaví Fjord, Chilean
842 Patagonia), J. Geophys. Res. Biogeosciences, 124(9), 2851–2865,
843 doi:10.1029/2019JG005028, 2019.
844 Watson, A. J.: Volcanic iron, CO2, ocean productivity and climate, Nature,
845 doi:10.1038/385587b0, 1997.
846 Weinbauer, M. G., Guinot, B., Migon, C., Malfatti, F. and Mari, X.: Skyfall - neglected
847 roles of volcano ash and black carbon rich aerosols for microbial plankton in the ocean, J.
848 Plankton Res., 39(2), 187–198, doi:10.1093/plankt/fbw100, 2017.
849 Welschmeyer, N. A.: Fluorometric analysis of chlorophyll a in the presence of chlorophyll
850 b and pheopigments, Limnol. Oceanogr., 39(8), 1985–1992,
851 doi:10.4319/lo.1994.39.8.1985, 1994.
852 Witham, C. S., Oppenheimer, C. and Horwell, C. J.: Volcanic ash-leachates: a review and
853 recommendations for sampling methods, J. Volcanol. Geotherm. Res., 141(3), 299–326,
854 doi:10.1016/j.jvolgeores.2004.11.010, 2005.
855 Wolinski, L., Laspoumaderes, C., Bastidas Navarro, M., Modenutti, B. and Balseiro, E.:
856 The susceptibility of cladocerans in North Andean Patagonian lakes to volcanic ashes,
857 Freshw. Biol., 58, 1878–1888, doi:10.1111/fwb.12176, 2013.
858 Yevenes, M. A., Lagos, N. A., Farías, L. and Vargas, C. A.: Greenhouse gases, nutrients
859 and the carbonate system in the Reloncaví Fjord (Northern Chilean Patagonia):

https://doi.org/10.5194/os-2020-65
Preprint. Discussion started: 3 July 2020
© Author(s) 2020. CC BY 4.0 License.


860 Implications on aquaculture of the mussel, Mytilus chilensis, during an episodic volcanic
861 eruption, Sci. Total Environ., doi:10.1016/j.scitotenv.2019.03.037, 2019.
862